

NEXT Multi-Thruster Array Test - Engineering Demonstration

Michael J. Patterson^{*}, John Foster[†], Heather McEwen[‡], Eric Pencil[§], and Jonathan Van Noord^{**}
NASA Glenn Research Center, Cleveland, Ohio, 44135

Daniel Herman^{††}
QSS Group at the NASA Glenn Research Center, Cleveland, Ohio, 44135

A multi-thruster array test was executed at NASA Glenn Research Center, focusing on the characterization of individual thruster, and array, performance and behavior – as affected by the simultaneous operation of multiple ion thrusters; a key step in development of the NEXT ion propulsion system. The subject of this characterization effort was a four engineering model NEXT thruster array in a 3+1 flight-representative configuration where one thruster was dormant (a spare). This test was executed concurrent with detailed plasma environments and plume measurements documented elsewhere. The array was operated over a broad range of conditions including the simultaneous firing of 3 thrusters at 20.6 kW total input power, yielding a total thrust of about 710 mN, at 4190 seconds specific impulse and approximately 71 percent efficiency. Major findings from a series of tests include: the performance observed for a thruster during operation in an array configuration appears to be consistent with that measured during singular thruster operation with no apparent deleterious interactions; and, operation of 1 neutralizer to neutralize 2-or-more thruster beams appears to be a potentially viable fault-recovery mode, and viable system architecture with significant system performance advantages. Overall, the results indicating single thruster operations are generally independent of array configuration have potentially significant implications with respect to testing requirements and architectural flexibility for multi-thruster systems.

Nomenclature

DCA	=	Discharge Cathode Assembly
DCIU	=	Digital Control Interface Unit
FP	=	Full-Power, corresponding to approximately 6860 W into the thruster
GRC	=	Glenn Research Center
IP	=	Intermediate-Power, corresponding to approximately 2780 W into the thruster
Ja	=	Accelerator grid impingement current, mA
JPL	=	Jet Propulsion Laboratory
LP	=	Low-Power, corresponding to approximately 1120 W into the thruster
mN	=	milli-Newton
Mn	=	Neutralizer Flow Rate, sccm Xe
MTAT	=	Multi-Thruster Array Test
NCA	=	Neutralizer Cathode Assembly
NEXT	=	NASA's Evolutionary Xenon Thruster
Vg	=	Coupling voltage (neutralizer common-to-facility ground), volts
PAT	=	Performance Acceptance Test
P _{in}	=	Input power into thruster, W

^{*} Electrical Engineer, Space Propulsion Branch, 21000 Brookpark Road/Mail Stop 16-1, AIAA Member.

[†] Aerospace Engineer, Space Propulsion Branch, 21000 Brookpark Road /Mail Stop 16-1, AIAA Member.

[‡] Aerospace Engineer, Space Propulsion Branch, 21000 Brookpark Road /Mail Stop 301-3, AIAA Member.

[§] Aerospace Engineer, Space Propulsion Branch, 21000 Brookpark Road /Mail Stop 301-3, AIAA Member.

^{**} Aerospace Engineer, Space Propulsion Branch, 21000 Brookpark Road /Mail Stop 16-1, AIAA Member.

^{††} Aerospace Engineer, Space Propulsion Branch, 21000 Brookpark Road /Mail Stop 16-1, AIAA Member.

PMS	=	Propellant Management System
PPU	=	Power Processor Unit
RPA	=	Retarding Potential Analyzer (diagnostic probe)
T/C	=	Thermocouple
TRL	=	Technology Readiness Level

I. Introduction

THE NASA Glenn Research Center is responsible for the development of NASA's Evolutionary Xenon Thruster (NEXT) ion propulsion system. The objective of the NEXT project is to advance next generation ion propulsion technology to NASA Technology Readiness Level (TRL) 5, with significant progress towards TRL 6.^{††} The NEXT system consists of a high performance, 7-kW, ion thruster; a modular, high-efficiency 7-kW power processor unit (PPU); a highly flexible advanced xenon propellant management system (PMS); a lightweight engine gimbal; and key elements of a digital control interface unit (DCIU) including software algorithms.¹⁻⁴ This design approach was selected to provide future NASA science missions with the greatest value in mission performance benefit at a low total development cost. Technology validation and mission analysis results in Phase 1 indicated that the NEXT technologies have the capabilities that provide the expected benefits, and further development was warranted.⁵

A multi-thruster array test (MTAT) is important to address thruster and gimbal specific questions that may drive the configuration of these subsystems and other subsystems, as well as the configuration of a final multi-thruster system test to be executed at the completion of Phase 2. This test would involve the use of multiple engineering model (EM) NEXT ion thrusters, as well as laboratory power consoles and propellant feed systems to operate multiple thrusters simultaneously. The whole host of in-situ diagnostics implemented during the Phase I single string integration test⁶ would be applied for the execution of this test, including near- and far-field beam ion and charge-exchange environmental measurements. Planar and other plasma probes mounted to the thrusters, along with current and voltage measurements of the functional thrusters would provide insight into the impact of the multi-thruster environment on individual thruster performance and life. Probes installed at relatively large distances from the thruster would be used to measure relevant plume parameters to characterize multi-thruster-induced spacecraft environment effects. Results could then be compared to model predictions and form a database available to operational mission spacecraft engineers. Information from this test, in combination with modeling results and spacecraft configuration studies, would provide definition to thruster configuration, gimbal requirements, and multi-thruster array geometry for final system testing.

The MTAT was executed, with the engineering demonstration portion of the test focusing on the characterization of individual thruster, and array, performance and behavior – as affected by the simultaneous operation of multiple ion thrusters. The subject of this characterization effort is a four-NEXT thruster array in a 3 + 1 configuration where one thruster is dormant (a spare). The *engineering objectives* include the following:

- A. Document multi-thruster system performance (1 + 1, 2 + 1, 3 + 1), and provide data to predict array life time^{§§};
- B. Assess performance and life time implications of multi-thruster operations on individual thrusters, as a function of –
 - 1) Operating mode [start-up, throttling, steady state, shutdown, recycling]
 - 2) Gimbal angle [gimbal angle authority impacts on adjacent thrusters - performance, erosion, thermal - and implications for lateral separation sensitivities]
 - 3) Array configuration [thruster spacing, thruster/neutralizer clocking];
- C. Assess thermal interactions – document the impact of array operation on individual thruster temperatures;
- D. Examine alternative system modes and architectures –

^{††} For this project TRL 5 implies that new technology components have been developed to an engineering model level, have met the appropriate environmental acceptance levels, and have demonstrated a significant level of component life. TRL 6 requires system/subsystem model or prototype demonstration in a relevant environment. Integrated system testing will be conducted such that the subsystem hardware is incrementally operated together, building up test data and confidence as the hardware becomes available. Multi-thruster testing, in combination with modeling, will support development of electric propulsion system configurations for future mission users.

^{§§} Full system-level performance will be assessed during follow-on array testing which is to include engineering model PPU and PMS subsystem elements.

- 1) Assess efficacy of n-1, n-2 ... 1 neutralizer as a system operational fault recovery mode [feasibility of neutralizer cross-strapping]
 - 2) Assess efficacy of n-1, n-2 ... 1 neutralizer as a standard system architecture; and
- E. Assess impacts of multi-thruster operations on PPU and PMS subsystem performance [validate engineering model (prototype model for thruster) hardware compatibility with multi-thruster system configurations, during follow-on testing].

This paper summarized the results from the engineering demonstration portion of the multi-thruster array test. Details of plasma property measurements made during the execution of this test using the in-situ diagnostics can be found in companion publications.⁷⁻¹⁰

II. Array Configuration

The NEXT array consists of 4 engineering model (EM) NEXT ion thrusters (EM1, EM2, EM4, and EM5) all manufactured at NASA GRC. The configuration of the 3 active thrusters is as identified in Table 1; ‘New’ refers to previously untested hardware. The array nominal configuration is 3+1 geometry, with spacing and thruster locations as determined from a spacecraft design activity conducted in 2003 at JPL for a Titan orbiter mission using a NEXT ion propulsion system^{††}; the baseline thruster spacing is 0.64 m center-to-center from corner-to-corner [0.91 m center-to-center across the diagonal]. The NEXT array in this nominal configuration is shown in Figures 1 and 2.^{***} For these tests EM2 functioned as the dormant (‘flight-spare’) thruster. Laboratory propellant feed systems and laboratory power consoles were used to operate the individual thrusters. Vacuum facility 6 (VF6) at NASA GRC was used for all array testing.^{†††} The array assembly was installed into the facility in an orientation to allow firing of the thrusters along the long-axis of the facility.

The array electrical schematic is shown in Figure 3; the grounding configuration is shown in Figure 4. A mechanical schematic is shown in Figure 5.

Table 1. Configuration of Active EM Thrusters

Component/Assembly	EM1	EM4	EM5
DCA	New	New	New
NCA	New	New	New
Ion Optics [Beam Dia.]	Pre-Operated [40 cm]	Pre-Operated [36 cm ^{†††}]	New [40 cm]
Discharge Chamber	Pre-Operated	New	New
Thruster	Pre-Operated	New	New

The array has the following design aspects:

- The array is reconfigurable to accommodate a 1 + 1, 2 + 1 ... up to 4 + 1 thruster geometry [5 thrusters].
- All 4 thrusters can be articulated. One of the 4 thrusters [EM1] is articulated via in-situ via motors [range of about ±10 degrees]; the other thrusters have a larger range of about ±16 degrees, but require manual adjustment which necessitates an atmosphere/vacuum cycle of the test facility.
- All 4 thrusters can be translated with respect to each other, to change inter-thruster distance.
- The thrusters can be reinstalled with some rotation about their axes to permit investigations as to the impact of relative neutralizer position on thruster and array functionality. Each thruster and its corresponding bracket could be rotated 180 degrees to allow the neutralizer assemblies to be in either the outboard radial or the inboard radial location. The nominal configuration has each neutralizer positioned on the outboard radial

^{***} EM2 uses an un-perforated stainless steel dome in place of an accelerator electrode. In the center of the dome are diagnostics. The dome is electrically isolated from other surfaces of the thruster so that it can be biased during plasma tests. Under normal conditions, all electrical terminations in the cable bundle from EM2 thruster were terminated at the vacuum facility penetration, tied together, and electrically connected to the test facility to ensure all EM2 thruster surfaces were grounded.

^{†††} VF6 is a space simulation vacuum tank of 7.6 m diameter and 22.9 m length evacuated with 12 cryogenic pumps.

^{†††} The EM4 optics were manufactured with a 40 cm beam diameter, and used during a 2hr wear test. The optics were subsequently modified by attachment of Tantalum foil on the downstream surface of the accelerator electrode to reduce the effective beam diameter to 36 cm. This was done to investigate the efficacy of reducing the beam diameter to improve thruster performance and reduce outer-aperture wear; prototype model NEXT thrusters have subsequently been fabricated with 36 cm beam diameter optics.

location; this default orientation was assumed to yield the most insensitive array operation to individual neutralizer function.

- Static diagnostics (Langmuir probes, RPAs, and pressure sensors) were mounted from the array frame, in the inter-thruster region, and in-and-about the exit plane of the thrusters. An RPA and Langmuir probe were mounted to a domed surface simulating an ion optics assembly on EM2. A 360-degrees-of-rotation probe arm with Faraday probes was mounted through the center of the array structure and allow for mapping near-field ion current densities. More diagnostics detail is provided in companion publications, including the results of plume measurements obtained over the conditions investigated here.⁷⁻¹⁰

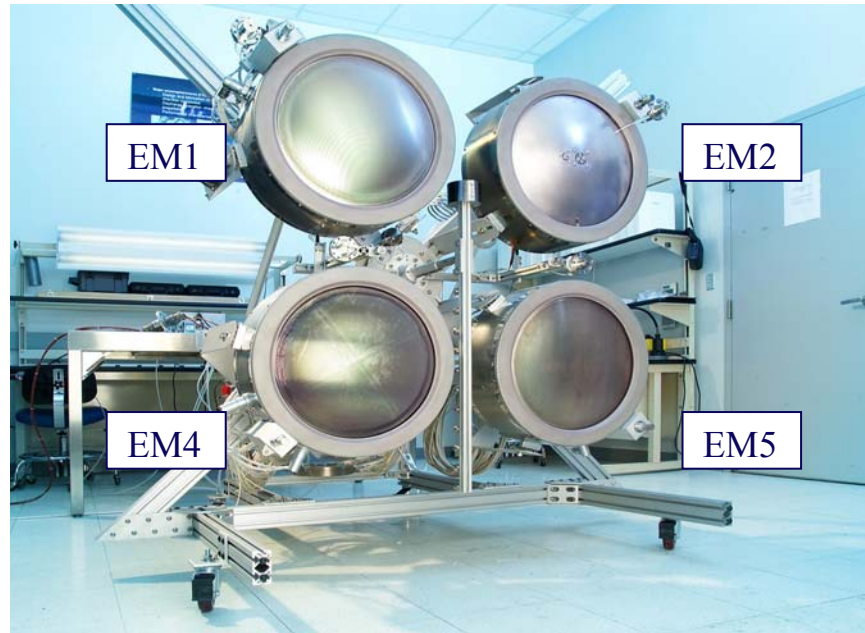


Figure 1. Three + one NEXT array.



Figure 2. Three + one NEXT array; array installed into VF6 test facility at NASA GRC. EM1 thruster is gimbaled.

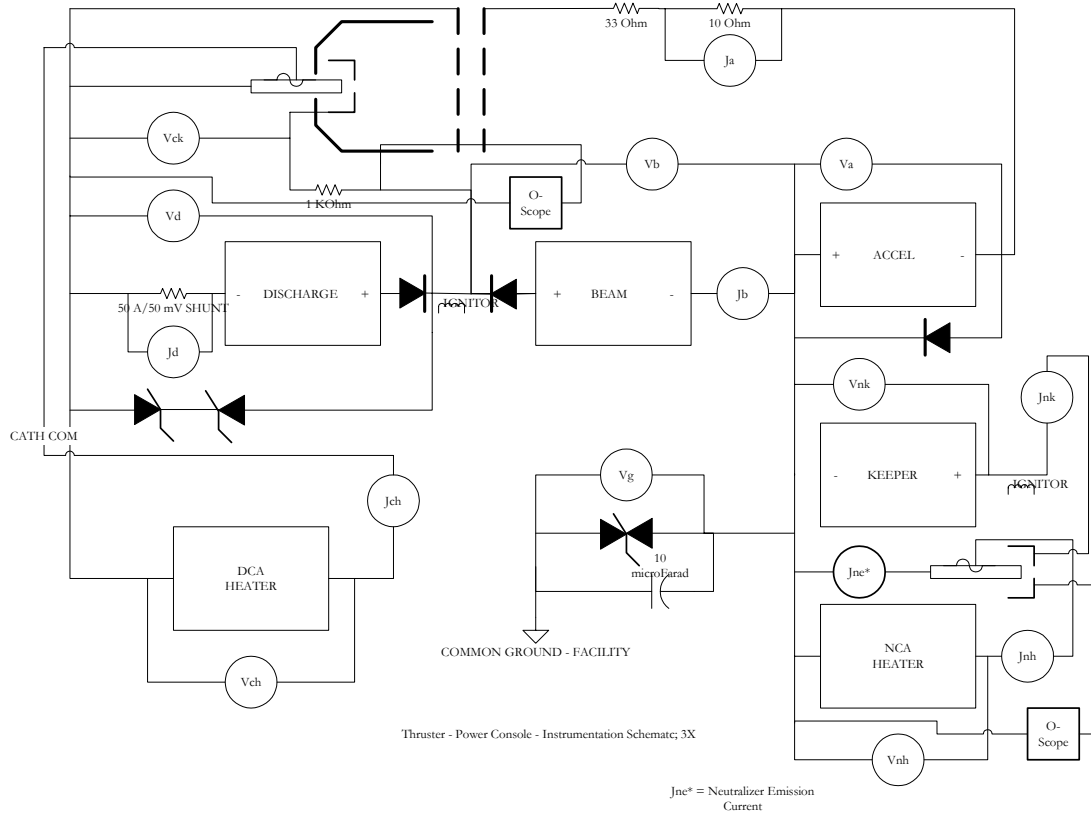


Figure 3. Thruster, power console, and instrumentation electrical schematic.

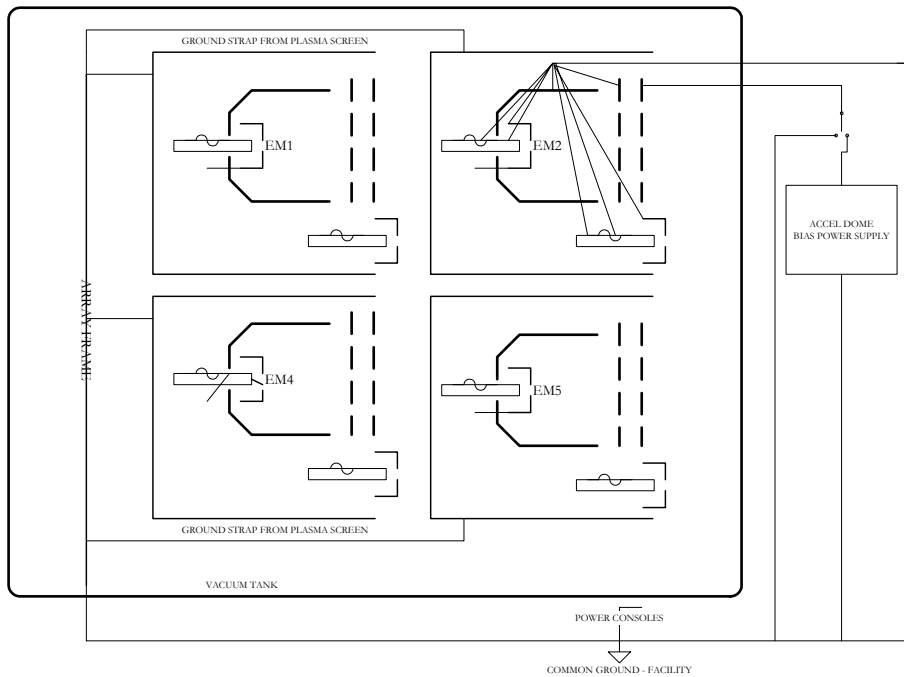


Figure 4. Grounding Configuration

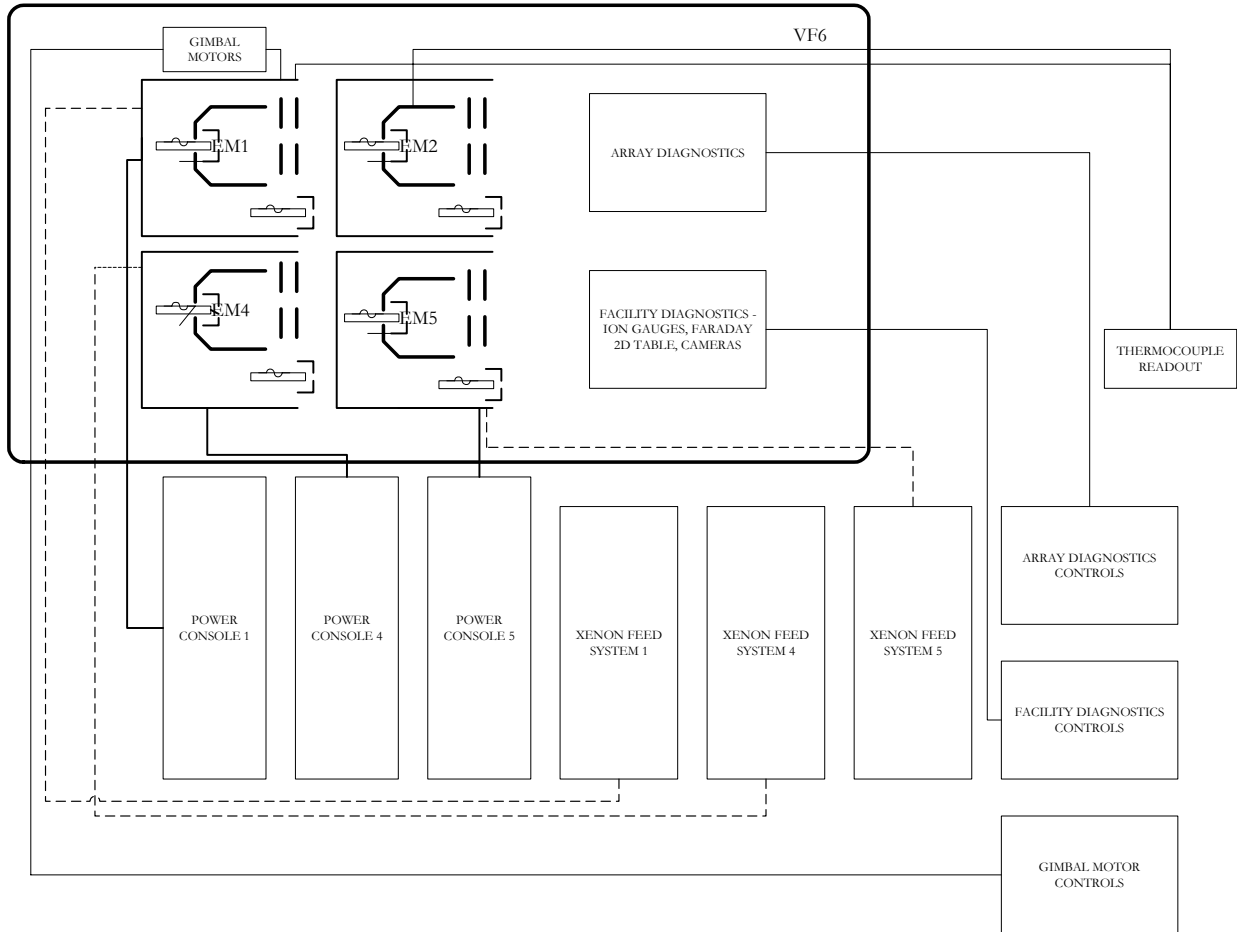


Figure 5. Mechanical Schematic

III. Engineering Demonstration

The following sections discuss the test results obtained, including performance, interactions, common neutralizer operations, and thermal data.

A. System Performance

One of the primary objectives of the MTAT was to document multi-thruster system performance (1 + 1, 2 + 1, and 3 + 1 thrusters), and provide data to predict array life time. To this end, initial tests were conducted to assess thruster performance (overall, ion optics, and neutralizer – a ‘PAT’) while operating in an array. System performance testing was executed in the following manner: the array was put into its nominal configuration; individual thrusters were started and throttled to full-power, an intermediate power level, and at a low power condition; at each condition the performance of individual thrusters was then documented. This was done additively. Data from the PATs of 1, 1 + 1, and 1 + 2 thruster configurations were documented and reviewed to determine array performance and this was compared to the nominal throttle table projections for individual thruster performance. An assessment of the impact of thruster spacing via assessment of EM1-EM4 tandem operation at 0.64 m spacing, versus EM1-EM5 tandem operation at 0.84 m spacing, was also conducted.

The system performance tests were conducted in the sequence identified in Table 2; individual thruster characterizations to establish baseline performance, and then, subsequently, additive tests of 2 and 3 thrusters.

Table 2. Multi-Thruster System Performance Test

Description of Test Sequence	Test
EM4 PAT @ LP, IP, and FP	TEST 1: Multi-Thruster System Performance
EM5 PAT @ LP, IP, and FP	
EM1 PAT @ LP, IP, and FP	
EM1+ EM5 PAT @ FP	
EM1+ EM4 + EM5 PAT @ FP	
EM1+ EM4 PAT @ FP	

As noted in Table 2, performance characterization tests were conducted on each individual thruster at LP, IP, and FP. This was followed by performance characterizations of the Array, with EM1 + EM5 (FP), EM1 + EM4 (FP), and EM1 + EM4 + EM5 (FP) configurations.

Noted here are some general observations of testing:

1. All thrusters (EM1, EM4, and EM5) functioned without issue. Similar results were obtained with propellant feed systems. Minor issues with the power consoles were experienced. However these were resolved quickly with only minor schedule and data impacts.
2. All thrusters operated with comparable performance, neutralizer operation, cathode ignitions, etc... Very minor unit-to-unit variability was observed, but is understandable in the context of minor hardware differences.^{§§§}
3. A ‘rapid’ thruster start-up process was defined, and repeatedly applied to all thrusters over the duration of the array testing.^{****} This process consisted of: (a) 15 minutes discharge operation at FP flow rates and cathode emission current, followed immediately by (b) beam extraction at FP. The thruster was (c) maintained at FP for 10 minutes, at which point (d) testing was initiated.
4. The thermal load imposed on the VF6 cryogenic pumps by the thruster ion beams from the array precluded operation of all 3 thrusters at FP for more than about 3-4 hours, at which point one or more pumps began to actively shed xenon which in turn would increase the indicated accelerator grid impingement current on thrusters (due to the local increase in neutral gas density and subsequent increase in charge-exchange ion current). This duration was however sufficient to conduct all testing, obtain diagnostics measurements, and yield performance data with the thrusters at thermal equilibrium. Operation of 3 thrusters at lower power levels, or 2 thrusters at FP could be conducted with indefinite duration without deleterious impact to the cryogenic pumps.

Sample array performance data for both 2- and 3-thruster configurations are documented in Table 3 obtained at thruster thermal equilibrium. Simultaneous operation of all active thrusters at FP resulted in approximately 20.6 kW total into the thrusters, producing a total thrust of about 711 mN, at an average specific impulse of about 4190 seconds at 70.8% efficiency. There was no demonstrable difference in EM1-EM4 operations (0.64 m center-to-center separation), as compared to EM1-EM5 operations (0.91 m center-to-center separation); i.e. - *there is no apparent impact of thruster-to-thruster spacing on thruster operation over the conditions investigated* (0.64 m – 0.91 m). Projected performance at FP operation, Table 4, taken from the baseline throttle table for the NEXT thruster, is shown for comparison.

§§§ For example, the accelerator grid impingement current on EM4 was slightly elevated as compared to the other thrusters, due to the mechanical modification made to the accelerator electrode to mask the diameter from 40 cm to 36 cm. Also reduced electron backstreaming margin for EM5 optics was observed, and can be attributed to slightly smaller inter-electrode cold gap. The reduced gap and lower neutral transparency (due to the pristine condition of the ion optics electrodes) also contributed to lower discharge losses on EM5 thruster.

**** It is likely a more rapid ignition and throttling of the NEXT thruster to FP could be achieved; the process outlined was simply established to standardize the method of testing, maximize repeatability, and execute the test expeditiously.

Table 3. Array Performance

Test Configuration/Thruster	Performance ^{†††}				
	P_{in}, W	Specific Impulse, Sec	Efficiency	Thrust, mN	Ja, mA
EM1 + EM5 PAT @ FP					
EM1	6850	4175	0.706	236	17.05
EM5	6820	4185	0.712	237	17.84
EM1 + EM4 PAT @ FP					
EM1	6870	4170	0.707	237	16.67
EM4	6875	4175	0.707	237	18.16
EM1 + EM4 + EM5 PAT @ FP					
EM1	6900	4195	0.708	238	21.67
EM4	6840	4170	0.706	236	23.82
EM5	6865	4195	0.711	237	21.25
EM1 + EM4 + EM5 PAT @ FP [Repeat test]					
EM1	6880	4185	0.707	237	21.74
EM4	6860	4175	0.705	237	22.92
EM5	6825	4180	0.711	237	22.66

Table 4. NEXT Projected Performance

NEXT Throttle Table	Performance				
	P_{in}, W	Specific Impulse, Sec	Efficiency	Thrust, mN	Ja, mA
EM Thruster	6860	4190	0.708	236	12.0

Elevated accelerator grid impingement currents due to charge-exchange ions were observed on each thruster, during multi-thruster operation, as noted in Table 3. However these appear to be largely, or entirely, attributable to an increase in local neutral density. Figure 6 plots accelerator grid impingement current versus beam voltage, for EM1 thruster; data obtained during perveance measurements. Currents were measured for several conditions:

- EM1 operation alone at FP;
- EM1 + EM4 operation at FP;
- EM1 + EM5 operation at FP;
- EM1 operation at FP with propellant flow (only) through EM4 thruster.

As indicated, the increase in accelerator grid impingement current experienced on EM1 thruster was approximately the same regardless of whether or not the secondary source in operation was EM4 at FP, EM5 at FP, or simply xenon propellant flow processed through EM4 thruster (at a rate necessary to establish an equivalent local pressure to FP EM4 thruster operation). *These data suggest that the increase in charge-exchange ion current on EM1 thruster during adjacent thruster operations is due to an increase in local neutral density (including facility effect contributions), and not migration of charge-exchange ion current created by adjacent thruster energetic beam ions.* As such, there is no apparent increase in charge-exchange current due to production of charge-exchange ions created by adjacent thruster operations. Also of note is that the charge-exchange current as measured on EM1

††† Performance of the thrusters was calculated by standard convention, using equations which account for items including NCA propellant flow and power consumed, as well as a correction to discharge chamber propellant efficiency for re-ingested propellant flow due to elevated facility pressure. A beam charge-state estimate is made (included in thrust-loss calculations) whose value is based on the discharge chamber propellant efficiency. The performance calculations assume there was no change in beam divergence between singular- and multiple-thruster operations, for a given thruster. This assumption is consistent with the beam divergence angles obtained from Faraday data for various test configurations which show no change in thruster beam divergence with test configuration.

thruster was essentially the same for EM1 + EM4 operation as compared to EM1 + EM5 operation, despite the significant difference in thruster spacing. Equivalent data are shown for 3-thruster operation in Figure 7, although the charge-exchange current correspondence between thruster operations and neutral propellant flow rate is not as precise.***

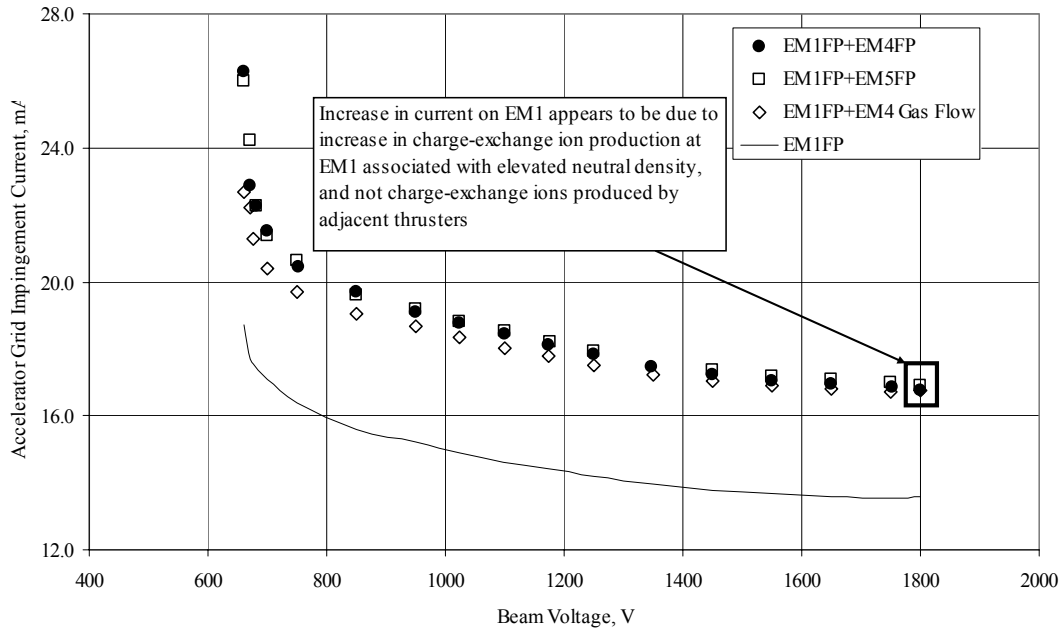


Figure 6. Accelerator grid impingement current vs. beam voltage; 2-thruster operation.

*** ‘EM1 FP + EM4 2x Gas Flow’ refers to operation of EM1 at FP, while a xenon gas flow sufficient to establish a local neutral pressure equivalent to that experienced during 3-thruster FP operation was processed through EM4 thruster. ‘EM1 FP + EM4 Gas Flow + EM5 Gas Flow’ refers to operation of EM1 at FP, while xenon gas flow necessary to establish a local neutral pressure equivalent to that experienced during 3-thruster FP operation was processed through both EM4 and EM5 thrusters.

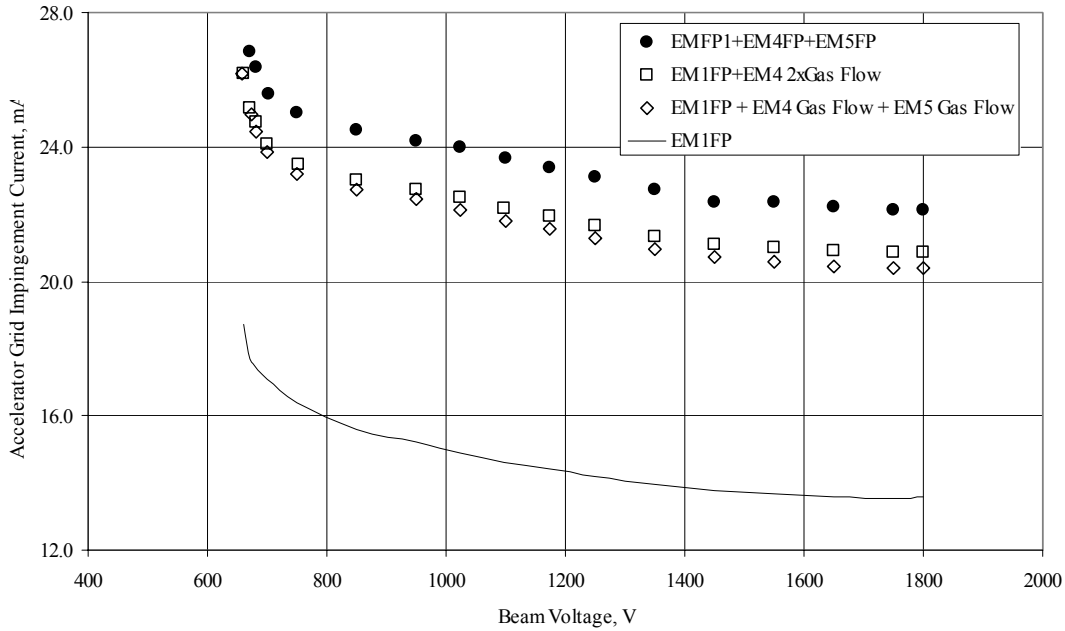


Figure 7. Accelerator grid impingement current vs. beam voltage; 3-thruster operation.

B. Thruster Interactions

The performance and life time implications of multi-thruster operations on individual thrusters were investigated as a function of operating mode [start-up, throttling, steady state, shutdown, recycling]. The impact of operating mode, reference Table 5, was examined by assessing the impact of startup, throttling, and shutdown of adjacent thrusters on EM1 thruster operation.

Table 5. Array Impact; Operating Mode

Description of Test Sequence	Test
EM1 PAT @ FP	TEST 2: Array Impact; Operating Mode
EM1 @ FP; EM4 startup, Operation @ FP	
EM1 + EM4 PAT @ FP	
EM1 @ FP; EM4 @ IP PAT	
EM1 + EM4 PAT @ FP	
EM1 + EM4 + EM5 PAT @ FP	
EM1 + EM5 PAT @ FP	

Data from these tests indicate that the operation of a thruster in an array does not appear to alter the performance of the thruster. This includes: overall performance, electron backstreaming, perveance, and neutralizer operation. Additionally there were no demonstrable thruster-to-thruster interactions during steady-state, and throttling, operations for 2- and 3-thruster array configurations. Approximately 10-20% of the total recycles (high-voltage arc conditions) however did appear to occur simultaneously on 2 thrusters. The cause of this was in determinant. The frequency of recycles was dependent upon thruster input power (increasing with input power), but independent of the number of operating thrusters. At all conditions the frequency was ≤ 1 recycle per hour.

Table 6 documents EM1 thruster performance as a function of test configuration. With the exception of the change in accelerator grid impingement current discussed previously, overall thruster performance for EM1 was constant and irrespective of array operation. Ion optics (electron backstreaming, and perveance) and neutralizer operation for EM1 was also constant and irrespective of array operation. Illustrated in Figure 8 is the EM1

neutralizer keeper voltage as a function of xenon flow rate, under conditions of singular and multi-thruster operations. No discernable change in neutralizer operation is identifiable.

Table 6. EM1 Thruster Performance

Test Condition	EM1 Performance				
	P_{in}, W	Specific Impulse, Sec	Efficiency	Thrust, mN	Ja, mA
EM1 PAT @ FP	6870	4185	0.707	237	12.18
EM1 + EM4 PAT @ FP	6870	4190	0.707	237	16.67
EM1 + EM5 PAT @ FP	6865	4185	0.708	237	17.53
EM1 + EM4 + EM5 PAT @ FP	6880	4185	0.707	237	21.74

Other than an increase in accelerator grid impingement current (which is at least partially due to facility pumping limitations) there is no indication that thruster parameters which control life processes are altered due to adjacent thruster function when a thruster is operated in an array configuration.^{§§§§} *Therefore thruster life established via singular thruster extended duration testing may accurately reflect thruster life when operated in an array configuration.* Facility effects associated with array function (increased propellant background pressure) likely will accelerate erosion processes experienced by individual thrusters in ground testing to levels above those experienced with single thruster operation, or to levels above those experienced during array operation in space-equivalent conditions.

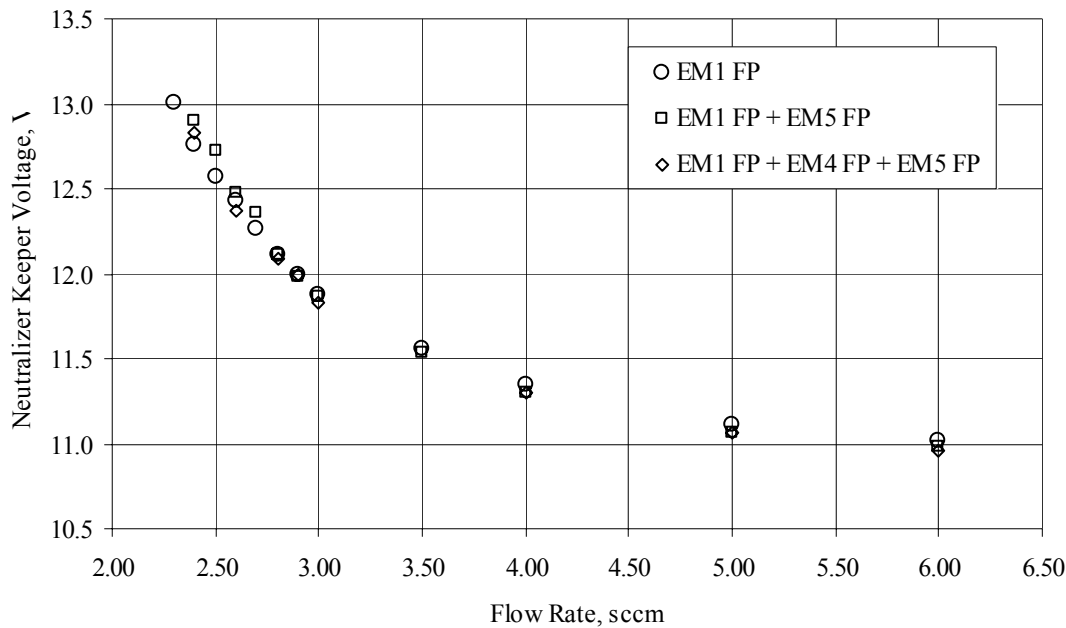


Figure 8. EM1 thruster neutralizer keeper voltage as a function of xenon flow rate.

The impact of gimbaling operations (sympathetic processes which may be related to thruster gimbaling angle) on thruster and array performance and function were also examined. This was executed in the manner detailed in Table 7, and involved the simultaneous FP operation of EM1 and EM5 thrusters, while EM1 thruster was articulated over a full range of motion.

The array was initially configured into its nominal orientation [gimbaling angle 0 degrees on all thrusters]. After both EM1 and EM5 thrusters were stable at FP and performance characterizations were completed, EM1 thruster

^{§§§§} Modest increases in magnet temperatures however are experienced due to adjacent thruster operations, as discussed later.

was then actively articulated in the radial direction and then the tangential direction (as illustrated in Figure 9) while operating. Performance measurements were obtained at each orientation. Subsequently EM1 thruster was returned to zero degrees gimbal angle, and the performance of both thrusters was re-characterized.

Table 7. Array Impact; Gimbal

Description of Test Sequence	Test
EM1 PAT @ FP; EM1 zero degrees gimbal angle	TEST 3: Array Impact; Gimbal
EM1 + EM5 PAT @ FP; EM1 zero degrees gimbal angle	
EM1 + EM5 PAT @ FP; EM1 radially-inboard 12.4 deg	
EM1 + EM5 PAT @ FP; EM1 radially-outboard 10.2 deg	
EM1 + EM5 PAT @ FP; EM1 tangentially-up 11.3 deg	
EM1 + EM5 PAT @ FP; EM1 tangentially-down 11.1 deg	
EM1 + EM5 PAT @ FP; EM1 zero degrees gimbal angle	

There was no discernable change in any thruster parameter for the actively-gimballed thruster (EM1) while firing at FP, nor any discernable change in adjacent thruster operation running at FP (EM5). This included no change in the measured accelerator grid impingement current for either active thruster. These data indicate that thruster gimbaling (approx. +/- 11degrees radially, and tangentially) does not alter, or impact the functionality of the thruster being actively gimballed, or the non-gimballed adjacent thruster for the configuration (inter-thruster center-to-center spacing of 0.91 m) investigated.

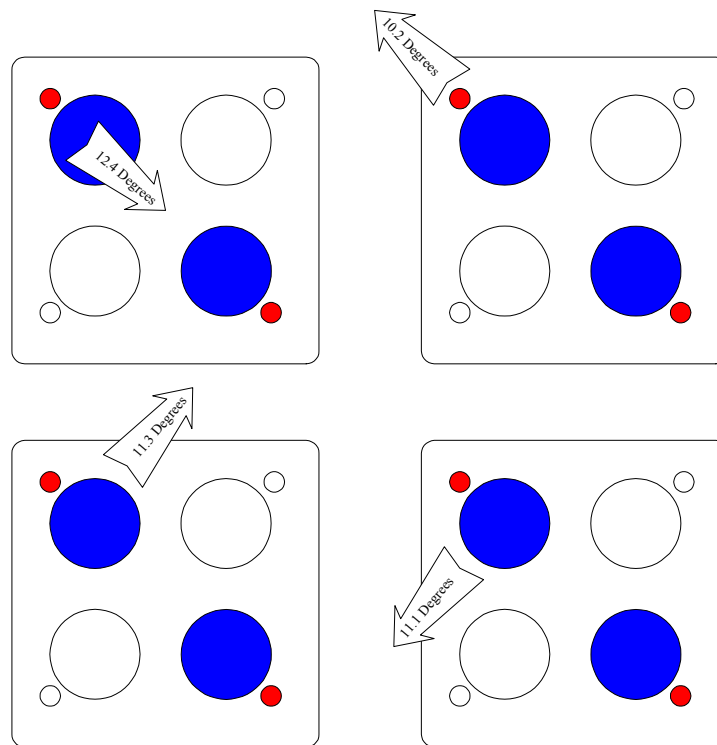


Figure 9. Test configuration and gimbal range for gimbaling test.

C. Shared- and Single-Neutralizer Operations

Alternative neutralizer architectures were examined. The efficacy of n-1, n-2 ... 1 neutralizer^{††††} as a system operational fault recovery mode, and as standard system architecture, was investigated. Tests included single-

^{††††} Where ‘n’ is the number of operational thrusters, or, separate ion beams.

neutralizer operation to simultaneously neutralize 2 or more ion beams, and use of one thruster's neutralizer to neutralize a 2nd thruster's ion beam ('cross-strapping').

The array was put into its nominal configuration; individual thrusters were started and throttled to full-power, an intermediate power level, and at the lowest power condition. At each condition the performance of individual thrusters was documented, including detailed characterizations of individual neutralizer functionality, and then individual neutralizers were eliminated from the array configuration subsequent to electrically shorting the neutralizer-common legs of the electrical circuit. Data were documented, and array and thruster performance with '2' operational neutralizers (with three operational thrusters, or n-1) and '1' operational neutralizer (both three and two operational thrusters, n-2 and n-1) were compared to that obtained with 'n' operational neutralizers. Data from a single thruster-operation (EM5) with a far-field neutralizer (EM1's) were compared to that obtained with a near-field neutralizer (EM5's). These shared- and single-neutralizer operations were conducted in the manner described in Table 8, and as illustrated in Figure 10. Neutralizer-commons between thrusters were configured as indicated in Figure 11, with switches to accommodate shorting during shared-neutralizer operations.

Table 8. Shared- and Single-Neutralizer Operations

Description of Test Configurations	Test
EM1 PAT @ LP, FP	TEST 4: Alternative Architectures; Neutralizer Sharing
EM1 + EM4 PAT @ FP	
EM1 + EM4 PAT @ FP with 1 neutralizer	
EM1 + EM5 PAT @ LP	
EM1 + EM5 PAT @ LP with 1 neutralizer	
EM5 @ LP with EM1 neutralizer	
EM1 + EM4 + EM5 PAT @ LP with 1 neutralizer	
EM1 @ FP + EM5 @ LP with 1 neutralizer	
EM1 + EM5 PAT @ FP with 1 neutralizer	

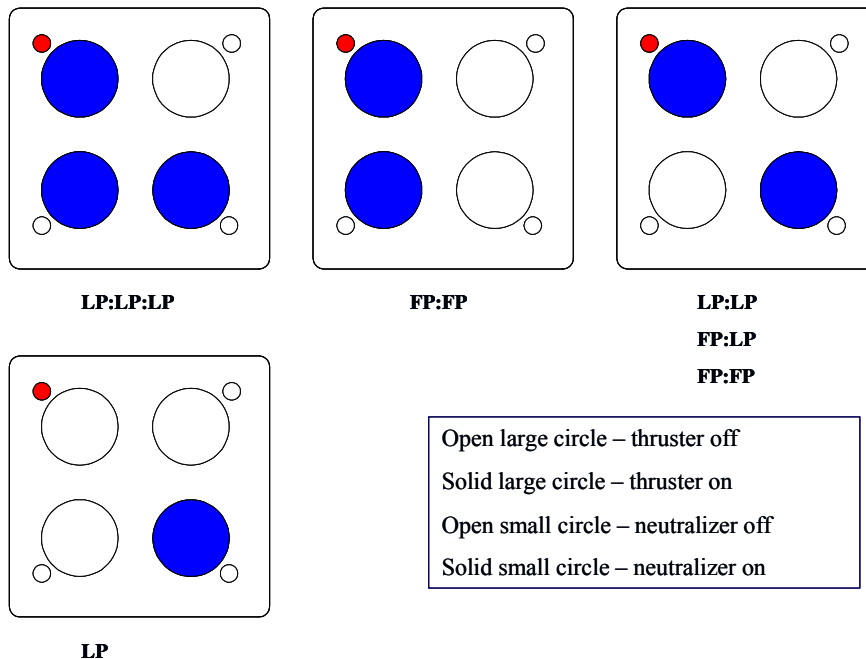


Figure 10. Shared and single-neutralizer operation test configurations; thruster power levels are indicated.

Single-neutralizer operation for 2- and 3-thruster beams had no discernable negative impact to thruster functionality, with only a very minor increase (~ 1 V) in the magnitude of coupling potentials (V_g). Figure 12 shows the neutralizer keeper voltage for EM1 thruster neutralizer as a function of xenon flow rate, under conditions where it was neutralizing a single thruster (EM1) and two thrusters (EM1 and EM5), for both LP and FP operation. Neutralizer functionality appears to improve with multiple-beam operations, due presumably to the increase in local plasma density and low energy ions as the neutralizer emission current is increased.

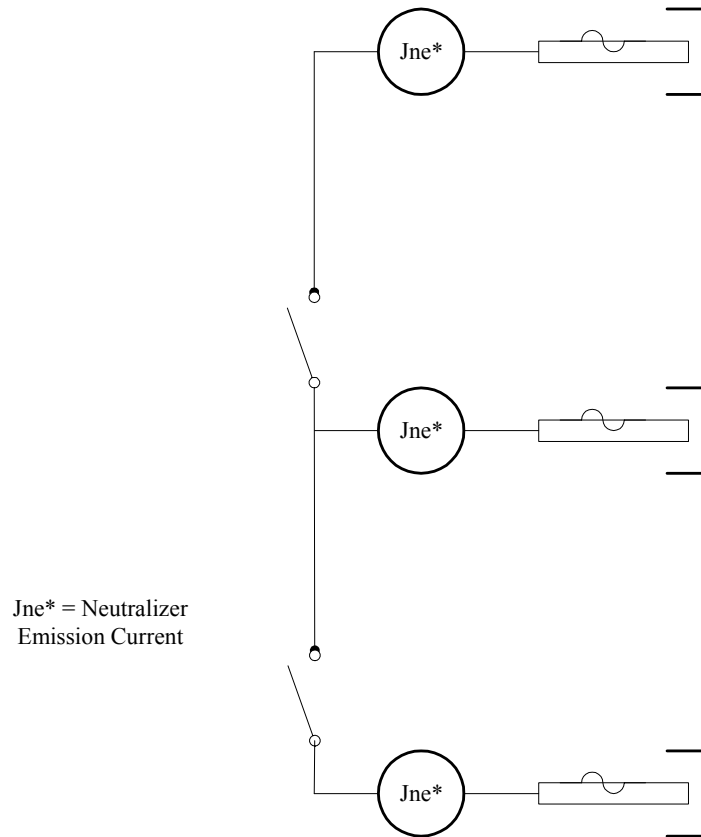


Figure 11. Neutralizer electrical configuration.

Start up and beam extraction of the 2nd and 3rd thrusters was demonstrated using a single (1st thruster's) neutralizer, with no discernable impact on functionality. Additionally, there was no change (re-distribution) of neutralizer emission currents when neutralizer-commons were electrically tied together while 2 or 3 thrusters were simultaneously operating using their individual neutralizers. As such there is likely no issue associated with starting multiple neutralizers with commons electrically tied together and hence no corresponding requirement for switching on the neutralizer-common leg in the PPU.

Single neutralizer operation yields significant improvements in 2nd ... nth thruster performance, particularly at low power levels. In Table 9, single neutralizer operation of 3 thrusters all at LP, an 11-13 percentage point increase in thruster efficiency, and a ~ 400 second increase in specific impulse for the 2nd and 3rd thrusters was demonstrated. Tables 10 and 11 quantify thruster performance for a 2 thruster array (with and without shared neutralizer) for LP and FP operation respectively. As noted in Table 11, a 7 percentage point increase in thruster efficiency, and a ~ 300 second increase in specific impulse for the 2nd thruster was demonstrated at FP by operation of a single neutralizer.

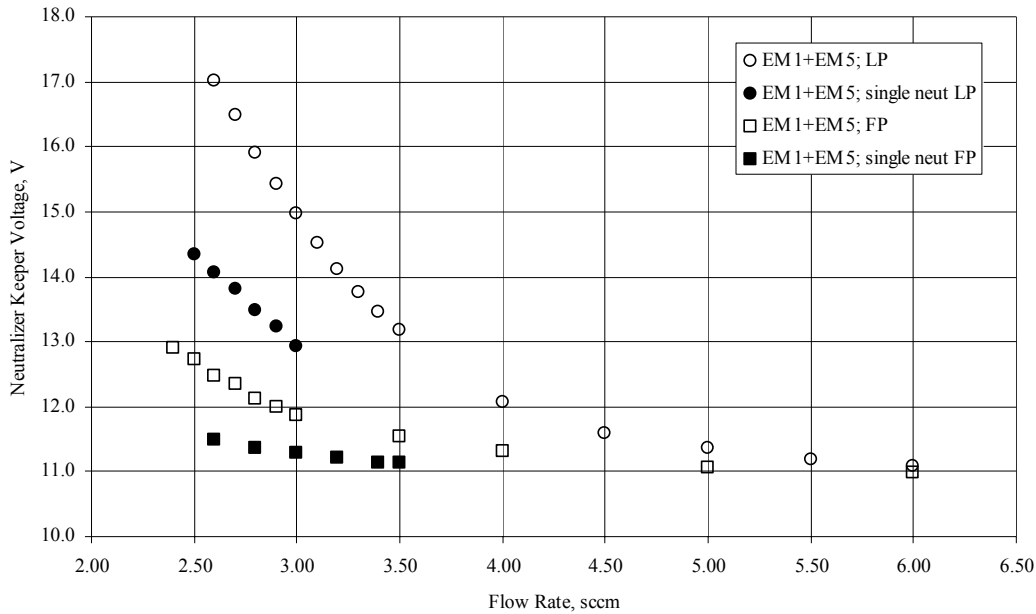


Figure 12. Neutralizer keeper voltage as a function of xenon flow rate; single and dual thruster beam neutralization.

Cross-strapping data is shown in Figure 13. Shown in this figure is the neutralizer keeper voltage as a function of xenon flow rate for the EM5 neutralizer neutralizing the EM5 thruster beam, and the EM1 neutralizer neutralizing the EM5 thruster beam (an increase of 0.91 m radial distance from neutralizer-to-beam, reference Figure 14). These data were obtained at LP; 1.20 A beam current. As indicated the EM1 neutralizer operated at lower keeper voltages than the EM5 neutralizer. The EM1 neutralizer operated at lower keeper voltages (and lower input power) as compared to EM5 neutralizer due to a subtle manufacturing difference between the EM1 and EM5 assemblies. The coupling voltage (V_g , voltage between neutralizer-common and facility ground) for EM1 neutralizer with EM5 thruster was of the order of -8 to -9 V over the range of indicated flow rates; comparable to that of the EM1 neutralizer with EM1 thruster. These data suggest that large (radial) repositioning of the neutralizer within the array over the range investigated is of negligible consequence with respect to its capacity to beam neutralize, and in fact subtle differences in as-built geometry are more dominant.

All these data indicate that *operation of 1 neutralizer to neutralize 2-or-more thruster beams appears to be a potentially viable fault-recovery mode, and viable system architecture with significant performance, configuration, and testing advantages.***** As such flight thruster array configurations that accommodate common sharing of neutralizers within the power processors to allow for single-neutralizer and/or cross-strapping operations may be warranted.

**** Operation of 3 thrusters at FP on a single neutralizer was not considered a likely flight mode since no near-term missions would have sufficient power to operate 3 NEXT thrusters at FP. Additionally the NEXT neutralizer maximum emission current is of the order of 13 A, which would be exceeded at this condition (3.0 A keeper current + 3.52 A beam current x 3 thrusters). However all data indicate that a single neutralizer can neutralize multiple thruster beams, up to its intended maximum emission current.

Table 9. Three-Thruster Array Performance - Single Neutralizer, LP Operation

EM1 + EM4 + EM5 PAT @ LP with 1 neutralizer	Performance					
	P _{in} , W	Specific Impulse, Sec	Efficiency	Thrust, mN	Mn, sccm	Vg
EM1	1105	2445	0.535	49.2	3.00	-11.98
EM4	1060	2845	0.649	49.2	0.00	
EM5	1035	2860	0.667	49.2	0.00	

Table 10. Two-Thruster Array Performance - LP Operation

EM1 + EM5 PAT @ LP	Performance					
	P _{in} , W	Specific Impulse, Sec	Efficiency	Thrust, mN	Mn, sccm	Vg
EM1	1120	2450	0.530	49.3	3.00	-8.76
EM5	1085	2460	0.548	49.3	3.00	-9.24
EM1 + EM5 PAT @ LP with 1 neutralizer	P _{in} , W	Specific Impulse, Sec	Efficiency	Thrust, mN	Mn, sccm	Vg
EM1	1115	2450	0.532	49.3	3.00	-10.28
EM5	1050	2865	0.661	49.2	0.00	

Table 11. Two-Thruster Array Performance - FP Operation

EM1 + EM5 PAT @ FP	Performance					
	P _{in} , W	Specific Impulse, Sec	Efficiency	Thrust, mN	Mn, sccm	Vg
EM1	6925	4215	0.712	238	4.01	-10.23
EM5	6835	4190	0.711	237	4.01	-10.75
EM1 + EM5 PAT @ FP with 1 neutralizer	P _{in} , W	Specific Impulse, Sec	Efficiency	Thrust, mN	Mn, sccm	Vg
EM1	6850	4190	0.708	236	4.00	-11.25
EM5	6795	4500	0.768	237	0.00	

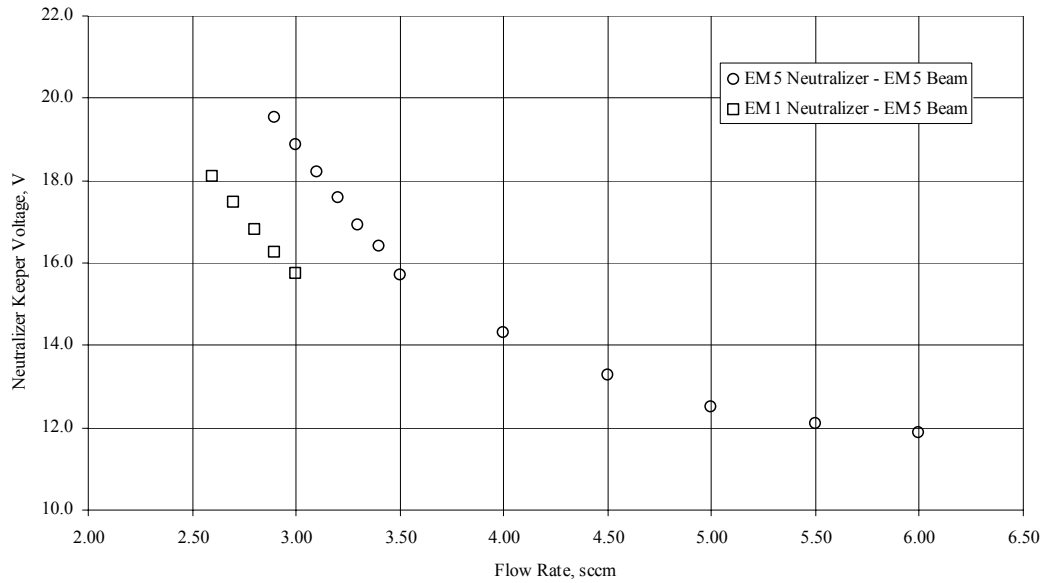


Figure 13. Neutralizer keeper voltage as a function of xenon flow rate; cross-strapping of EM1 neutralizer with EM5 thruster, LP operation.

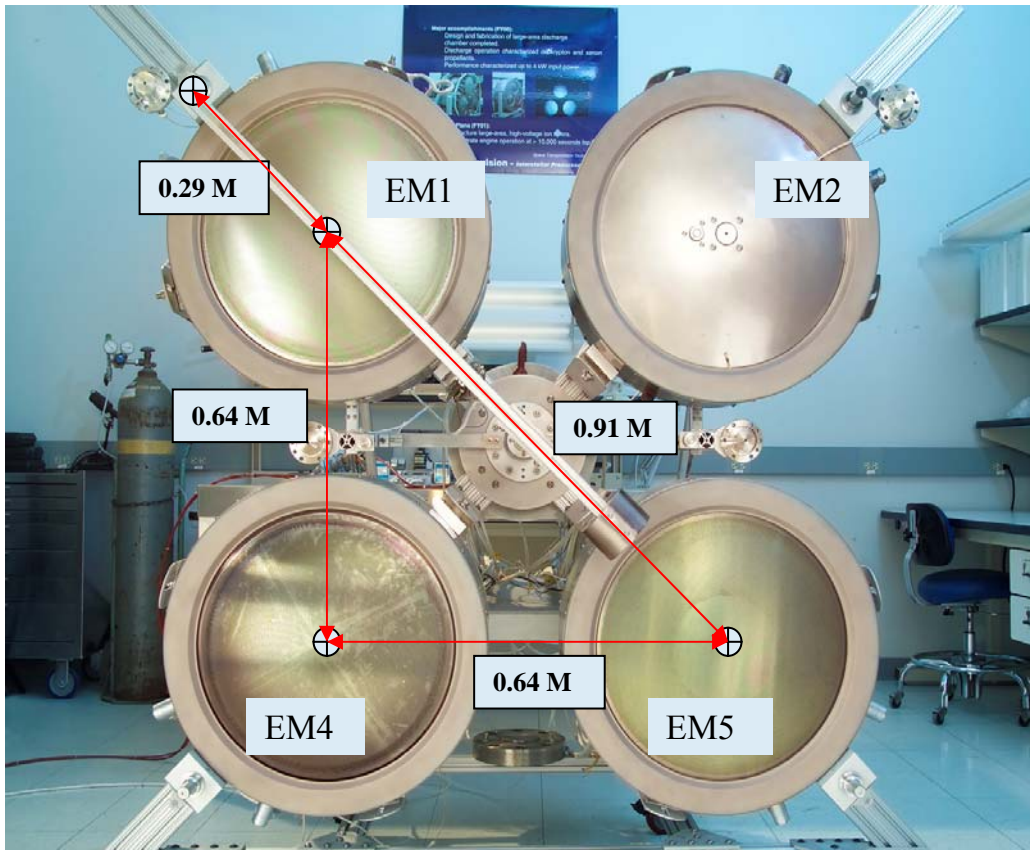


Figure 14. Array geometry; spacing noted in meters.

D. Thermal Interactions

Five type-K thermocouples (T/Cs) were installed on the thrusters on the array to document temperatures during operation; one on EM1 thruster, and 4 on EM2 dormant thruster. The locations of the T/Cs are as illustrated in Figure 15, and are identified below:

T/C 1: EM1 thruster plasma screen external surface; vertical bottom, 15.24 cm behind plane of front mask on the exterior surface of the cylindrical portion;

T/C 2: EM2 thruster front (optics end) magnet ring;

T/C 3: EM2 thruster middle magnet ring;

T/C 4: EM2 thruster cone magnet ring;

T/C 5: EM2 thruster back magnet ring; T/C 2-5 all located azimuthally 15 degrees from vertical bottom, 150 degrees clockwise from neutralizer assembly.

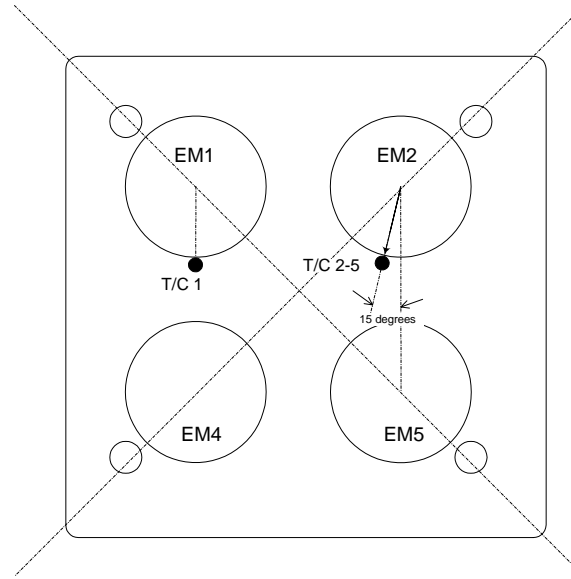


Figure 15. Locations of thermocouples on the array as viewed head-on.

Data from the 5 T/Cs (1 on EM1 thruster, 4 on the dormant EM2 thruster) were recorded during array testing, and are summarized here. Operation of 1, 2, and 3 thrusters, all at FP, was conducted on several occasions. Temperature data for this configuration are shown in Figure 16 and 17, and corresponding input power conditions are identified in Table 12. Initial T/C temperatures for both thrusters prior to application of power were 0 to -1 degrees C. Discharge ignition for EM1 occurred at 0623 hours, with operation at FP beginning 0650 hours. EM5 was throttled to FP at 0728 hours. EM4 was throttled to FP at 1136 hours. Temperature on EM1 and EM2 asymptote to ~106 deg C and ~10 deg C respectively after approximately 2.5 hours of multi-thruster operations at FP. Data for T/Cs 2-5 are repeated on Figure 17 with an expanded scale, which indicates that peak temperatures on the dormant thruster EM2 are experienced from front-to-back/maximum-to-minimum.

Figures 18 and 19 display the equilibrium temperatures obtained on EM1 and EM2 thrusters as a function of test configuration. Initial temperatures for both thrusters prior to application of power were 0 to -1 degrees C. As indicated from the two figures, not surprisingly operation of EM5 thruster had the least impact on EM1 thruster temperatures, and correspondingly EM4 on EM2. Both EM1 and EM2 thrusters experienced the highest temperatures of course when all active thrusters in the array were running at full power. EM1 thruster (plasma screen) temperature increased by roughly 10 degrees C from those observed during FP operation of EM1, for every additional active thruster operated at FP. EM2 thruster magnet temperatures (front magnet ring) increased by about 7 degrees C for each active array thruster operating at FP. *None of the observed increases in thruster temperatures resulting from array operations are large enough in magnitude to be of concern since there is substantial thermal margin on all key thruster components at FP.* §§§§§

§§§§§ Recent performance acceptance testing of a prototype-model NEXT thruster (higher mechanical and thermal integrity than that of the EM NEXT thruster) indicates greater than 60 degree C margin at FP for single-thruster operations under ambient conditions.

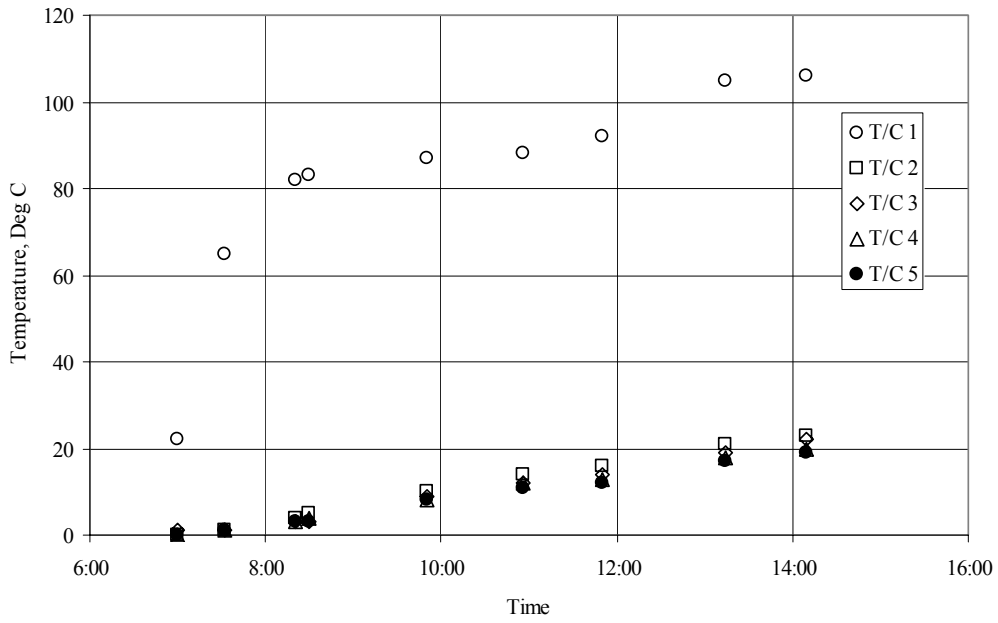


Figure 16. EM1 and EM2 thruster equilibrium temperatures during multi-thruster operations at FP.

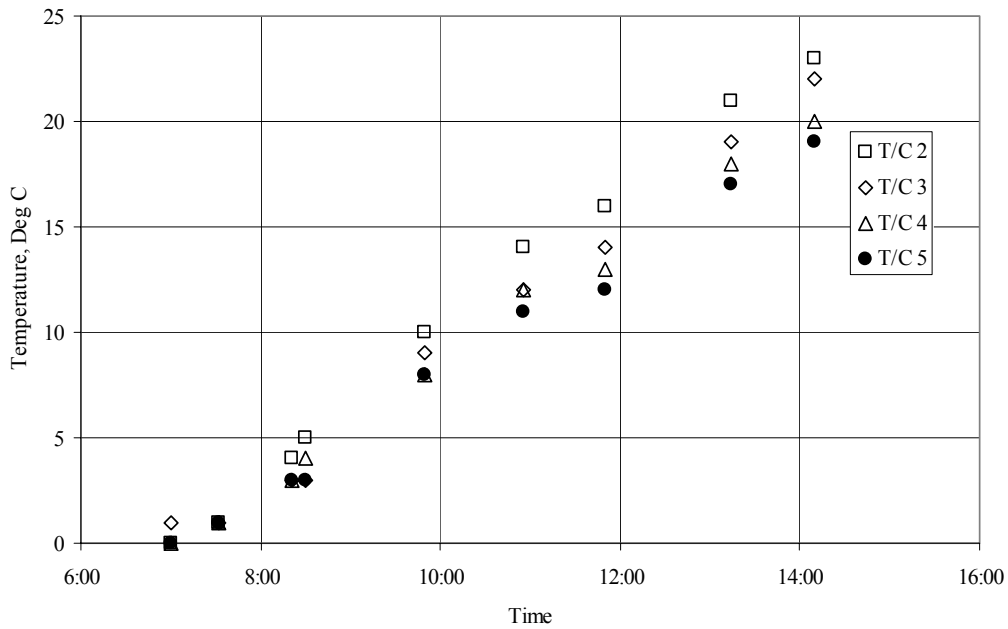


Figure 17. EM2 thruster equilibrium temperatures during multi-thruster operations at FP.

Table 12. Full-Power Multi-Thruster Operations

Time	Test Condition
07:00	EM1 @ FP
07:32	EM1 + EM5 @ FP
08:21	EM1 + EM5 @ FP
08:30	EM1 + EM5 @ FP
09:50	EM1 + EM5 @ FP
10:56	EM1 + EM5 @ FP
11:50	EM1 + EM4 + EM5 @ FP
13:15	EM1 + EM4 + EM5 @ FP
14:10	EM1 + EM4 + EM5 @ FP

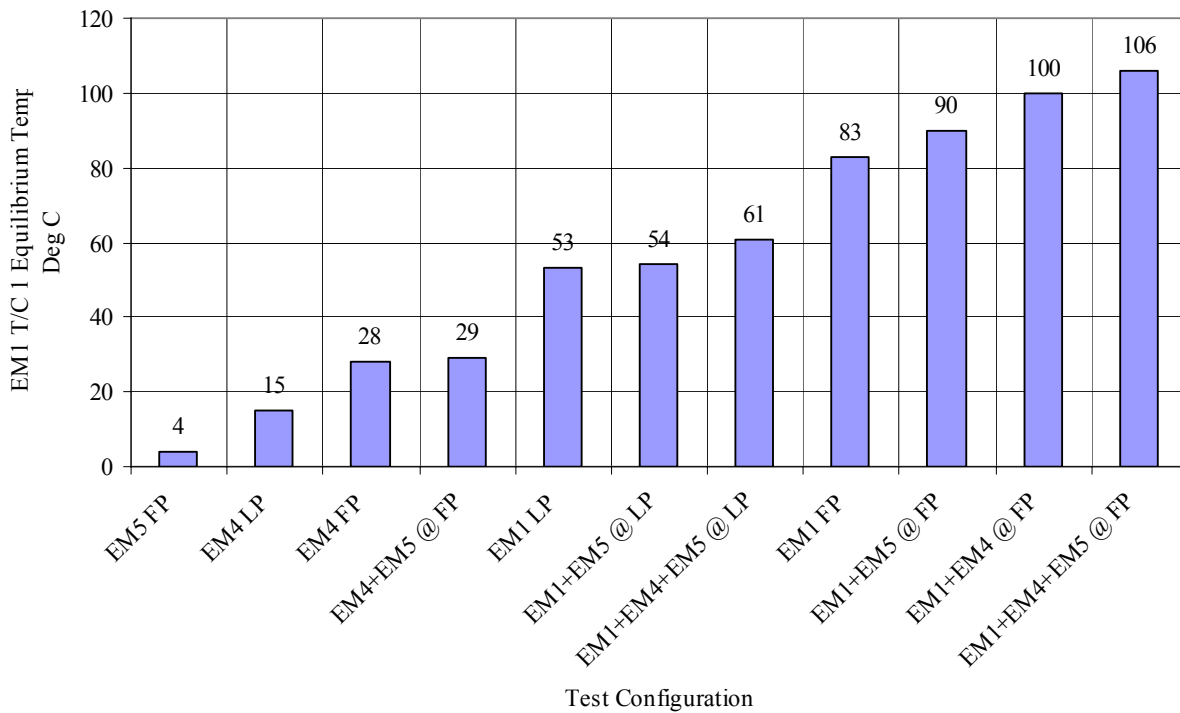


Figure 18. EM1 thruster T/C1 equilibrium temperatures as a function of test configuration.

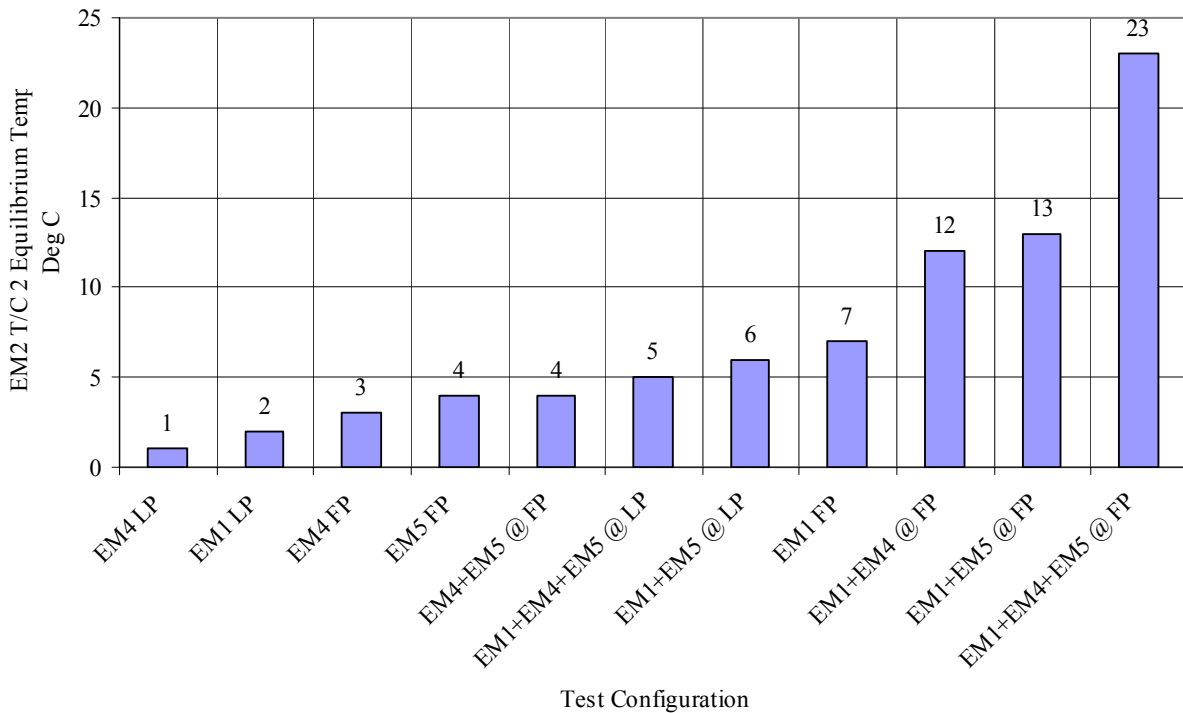


Figure 19. EM2 thruster T/C2 equilibrium temperatures as a function of test configuration.

IV. Conclusion

A multi-thruster array consisting of 4 engineering model NEXT ion thrusters was assembled and tested at NASA GRC. The array was tested over a range of operating conditions and different system configurations to investigate the effect of the simultaneous operation of multiple ion thrusters on individual thruster performance and life, and quantify the performance of the array. A variety of tests were conducted to examine system performance, thruster interactions, and shared- and single-neutralizer operations. Thermal data were also documented for individual thrusters operating in the array.

The performance observed for a thruster during operation in an array appears to be consistent with that measured during singular thruster operation. That is, operation of a thruster in an array does not appear to alter the performance of the thruster. There is no apparent impact of thruster-to-thruster spacing on thruster operation, over the range investigated. Also there are no demonstrable thruster-to-thruster interactions during steady-state, or throttling for 2- and 3-active thrusters in an array configuration. By extension, these findings suggest that the performance and life of an array can be established from testing of individual thrusters. There was also no discernable change in thruster parameter during gimbaling for the actively-gimballed thruster while firing, nor any change in adjacent thruster operation.

Single-neutralizer operation to simultaneously neutralize 2 or more ion beams, and using one thruster's neutralizer to neutralize a 2nd thruster's ion beam were examined. Operation of 1 neutralizer to neutralize 2-or-more thruster beams appears to be a viable fault-recovery mode, and viable system architecture, with no discernable impact on thruster functionality. Single-neutralizer operation for 2 thruster beams had no discernable negative impact, with very minor increase in coupling potentials. Single neutralizer operation yields significant improvements in 2nd ... nth thruster performance; 11-13 percentage point increase in thruster efficiency, and 400 sec increase in specific impulse at 1 kW. Start up and beam extraction of 2nd and 3rd thrusters was demonstrated on a single (1st thruster's) neutralizer, with no discernable impact. Operation of 1 neutralizer on one thruster to neutralize a thruster beam from a different thruster also appears to be a viable fault-recovery mode with no discernable impact. These data indicated that there may be significant architectural flexibility regarding approaches to beam neutralization of array configurations, which may also provide for improvements in overall system performance as compared to 1-thruster/1-neutralizer geometries.

Acknowledgments

The authors would like to acknowledge the support of the In-Space Propulsion program managed by the NASA Marshall Space Flight Center.

References

- ¹Frandina, M., Carpenter, C., Soulas, G., Snyder, A., and Patterson, M., "Status of the NEXT Ion Engine Life Test," AIAA-2005-4065, Joint Propulsion Conference, July 2005.
- ²Todd, P. Wiseman, S., Martinelli, R., and Pinero, L., "Status of the NEXT 7 kW Power Processing Unit," AIAA-2005-3868, Joint Propulsion Conference, July 2005.
- ³Hoskins, W., Polaha, J., Hobson, D., Soulas, G., Patterson, M., Sovey, J., and Talerico, L., "Overview of the NEXT Ion Propulsion System Program at Aerojet," AIAA-2005-3885, Joint Propulsion Conference, July 2005.
- ⁴Monheiser, J., Aadland, R., and Wilson, F., "Development of a Ground Based Digital Control Interface Unit (DCIU) for the NEXT Propulsion System," AIAA-2004-4112, Joint Propulsion Conference, July 2004.
- ⁵Benson, S., Patterson, M., Vaughan, D., Wilson, A., and Wong, B., "NASA's Evolutionary Xenon Thruster (NEXT) Phase 2 Development Status," AIAA-2005-4070, Joint Propulsion Conference, July 2005.
- ⁶Patterson, M.J., Pinero, L., Aadland, R., and Komm, D., "NEXT Ion Propulsion System: Single-String Integration Test Results," JANNAF Conference, May 2004.
- ⁷Pencil, E.J., Foster, J.E., Patterson, M.J., Diaz, E., Van Noord, J., and McEwen, H., "Ion Beam Characterization of NEXT Multi-Thruster Array Plume," AIAA-2006-5182, 42nd Joint Propulsion Conference and Exhibit, Sacramento, CA, July 2006.
- ⁸Foster, J.E., Pencil, E., Patterson, M.J., McEwen, H., Diaz, E., and Van Noord, J., "Plasma Characteristics Measured in the Plume of a NEXT Multi-Thruster Array," AIAA Paper 2006-5181, 42nd Joint Propulsion Conference and Exhibit, Sacramento, CA, July 2006.
- ⁹McEwen, H., Foster, J.E., Pencil, E., Patterson, M.J., Diaz, E., and Van Noord, J., "Characterization of Plasma Flux Incident on a Multi-Thruster Array," AIAA Paper 2006-5183, 42nd Joint Propulsion Conference and Exhibit, Sacramento, CA, July 2006.
- ¹⁰Foster, J.E., Pencil, E., McEwen, H., Patterson, M.J., Diaz, E., and Van Noord, J., "Neutralizer Plasma Coupling in a NEXT Multi-thruster array", AIAA Paper 2006-5184, 42nd Joint Propulsion Conference and Exhibit, Sacramento, CA, July 2006.
- ¹¹Oberto, R., et al., "Advanced Projects Design Team, Titan Orbiter 2003-10," JPL Report ID #658, 2003.